Output characteristics analyses of a novel dual-slab laser with an off-axis one-sided stable-unstable resonator

Lingling Zhang (张玲玲), Junqing Meng (孟俊清), Yan Huang (黄 燕), and Qiquan Hu (胡企铨)

Shanghai Institute of Optics and Fine Mechanics, Chinese Academy of Sciences, Shanghai 201800

Received August 30, 2005

A novel dual-slab laser with an off-axis one-sided stable-unstable resonator which can compensate for thermal distortion to some extent by flipping the optical beam is described in this paper. The output power, efficiency, and near-field and far-field intensity distributions of the dual-slab laser have been studied. The results indicate that the novel dual-slab laser has better performance than the normal dual-slab laser with the same off-axis one-sided stable-unstable resonator.

OCIS codes: 140.0140, 140.3410, 140.4780.

Various applications in material processing require brightness large with output power in the kilowatts range. Previous attempts to build high-power, high-beam-quality lasers typically used a rod laser design with either end or side pumping. At high powers, however, thermal effects degrade laser performance. Rectangular shaped slabs provide a more favorable geometry for high power operation. However, high resonator Fresnel number of slab lasers caused by the large slab cross section results in multi-mode laser beams with high value for M^2 and spatial modulation of the power density distribution when using common stable resonator. To extract high quality beams from slab gain media, so-called off-axis unstable resonators are attractive, and such resonators have been successfully applied to solid-state lasers and carbon dioxide lasers[1−3]. Besides beam characteristics, a high overall efficiency is of the increasing importance for higher output powers. Therefore, in order to get the highest extract efficiency, it is important to optimize the design of a resonator. In this paper, a novel dual-slab laser is described, which can compensate for thermal distortion to some extent by flipping the optical beam[4].

Figure 1 shows the novel face-pumped, dual-slab laser. The temperature gradient is forced to be nearly one-dimensional by arranging the cooling and pumping properly. Focusing is eliminated in the x-direction by the uniformity of the pumping and cooling in that direction. To compensate the wavefront distortion in y-direction, two slabs with the same size, material, and performance are placed parallelly and pumped uniformly and symmetrically from x-z plane of each slab by the same power pumping source. The both faces of each slab were cooled respectively using high cooling capability flowing coolant with different temperatures T_1 and T_2 ($T_1 > T_2$), as shown in Fig. 1. A reflecting system composed of M_3—M_5 can flip the laser beams, make them symmetrically travel along the higher temperature side of one slab through the lower temperature side of the other slab. By this way, the wavefront distortion caused by the non-uniform temperature distribution of the laser gain media slab will be self-corrected.

The resonator, as shown in Fig. 2, is composed of two highly reflecting cylindrical mirrors M_1 and M_2. In the horizontal plane a confocal off-axis one-sided unstable positive-branch resonator is formed by the concave and convex surfaces of the mirrors. In the vertical plane, a flat-flat on-axis resonator is configured.

The unstable direction of an off-axis one-sided stable-unstable resonator, when viewed from the output coupler, is geometrically similar to a beam expanding telescope with a magnification equal to the ratio between the focal lengths of the end mirrors. Based on the original idea of Siegman[5], the lowest loss steady-state mode of such a resonator may be thought as consisting of a spherical wave with its center at the common focus travelling from the small mirror to the large mirror and a plane wave returning from the large mirror to the small mirror.

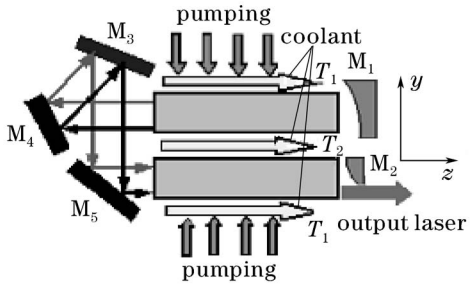

Fig. 1. Plan view of the face-pumped, dual-slab laser.

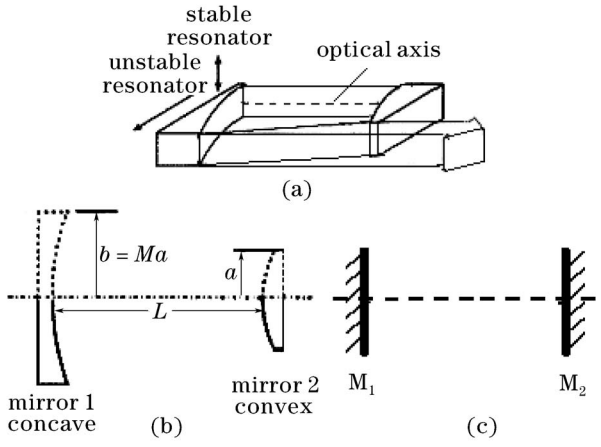

Fig. 2. (a) An off-axis stable-unstable hybrid resonator; (b) a positive branch unstable resonator; (c) a flat-flat resonator.

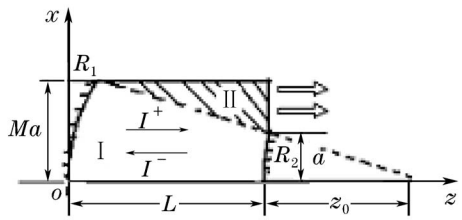

Fig. 3. Evaluation of the field intensity in off-axis one-sided unstable resonator.

We can easily see from Fig. 3 that within the region denoted by I, which is filled with the light beam travelling in both directions, the population inversion and intensity vary only along the z axis ($0 \le z \le L$), whereas these quantities are constant over the cross section.

The problem is formulated in the paraxial approximation, assuming homogeneous broadening of the laser line and a spatially homogeneous index of refraction. Let I^+ and I^- satisfy

$$\frac{\mathrm{d}I^+}{\mathrm{d}z} = I^+[g(z) - \alpha_0], \tag{1}$$

$$\frac{\mathrm{d}I^-}{\mathrm{d}z} - \frac{I^-}{z_0 + L - z} = -I^-[g(z) - \alpha_0], \tag{2}$$

where z is the direction of the field propagation, I^+ is the intensity of the resonator field in the z direction, I^- is the intensity in the opposite direction, the gain $g(z) = \frac{g_0}{1+(I^+ + I^-)/I_{\mathrm{sat}}}$ (g_0 is small signal gain, I_{sat} is the saturation intensity), α_0 is the absorption coefficient per transit.

Integrating Eqs. (1) and (2), the intensities I^+ and I^- are obtained as

$$I^+(z) = I^+(0) \exp\{\int_0^z [g(z') - \alpha_0]\mathrm{d}z'\}, \tag{3}$$

$$I^-(z) = I^-(0) \left(\frac{z_0 + L}{z_0 + L - z}\right) \exp\{-\int_0^z [g(z') - \alpha_0]\mathrm{d}z'\}. \tag{4}$$

Assuming that both mirrors are totally reflecting, the boundary conditions are given by

$$I^+(0) = I^-(0) = I(0), \tag{5}$$

$$I^+(L) = I^-(L). \tag{6}$$

According to Eqs. (3) and (4)

$$I^+(z)I^-(z) = I(0)^2 \frac{z_0 + L}{z_0 + L - z}. \tag{7}$$

According to Ref. [6], $[I^+(z) + I^-(z)]_{\min}/[I^+(z) + I^-(z)]_{\max} \approx 1$, therefore, within in a few percent, $I^+(z) + I^-(z)$ is equal to $2\sqrt{I^+(z)I^-(z)}$, larger distances are not encounted in numerical calculations

$$I^+(z) + I^-(z) \approx 2\sqrt{I^+(z)I^-(z)} = 2I(0)\sqrt{(z_0 + L)/(z_0 + L - z)}. \tag{8}$$

Substituting Eq. (8) into Eqs. (3) and (4), when $z = L$, we can obtain an equation for the determination of I_0 ($I_0 = I(0)/I_{\mathrm{sat}}$),

$$4I_0\sqrt{\frac{M}{M+1}} - 8I_0^2 \frac{M}{M-1} \ln \frac{\sqrt{M}(2I_0 + 1)}{2I_0\sqrt{M} + 1} = 1 - \frac{\ln\sqrt{M} + \alpha_0 L}{g_0 L}, \tag{9}$$

where $M = (z_0 + L)/z_0$ is the magnification of the resonator.

Let us now assume that α_0/L is sufficiently small that the paraxial approximation is good throughout region I as shown in Fig. 3. Then, as suggested in Ref. [7], after obtaining the distribution of $I^+(z)$ in the region I, we can calculate the distribution in the region denoted by II where $I^-(z) = 0$ by means of a suitable applicable equation to be a pure amplification regime[8]

$$\ln\left(\frac{I_{\mathrm{out}}}{I^+(z)}\right) = (g_0 - \alpha_0)(L - z) + \frac{g_0}{\alpha_0} \ln\left[\frac{g_0/\alpha_0 - 1 - I_{\mathrm{out}}}{g_0/\alpha_0 - 1 - I^+(z)}\right], \tag{10}$$

where $I^+(z)$ is the intensity at the entry into region II, I_{out} is the intensity at the exit from the resonator.

In the end, the total output power P_{out} can be calculated by

$$P_{\mathrm{out}} = \int_a^{Ma} I_{\mathrm{out}}(x) b \mathrm{d}x, \tag{11}$$

where $(Ma - a) \times b$ is the dimension of output aperture.

In our experiment, the dimension of the active medium Nd:glass is 20 × 100 × 500 (mm). In order to meet specific energy output requirements, the gain medium can be characterized when such laser is designed. The parametric evaluations involve determining the system's small signal gain coefficient g_0, constant loss coefficient α_0, and the saturation intensity I_{sat}, which are three critical parameters in determining the performance of a laser (power extraction, coupling, etc.). In this paper, the transcendental equations obtained by Schindler[9] were used to decide these parameters. Their values are $g_0 = 1.144\ \mathrm{m}^{-1}$, $\alpha_0 = 0.0676\ \mathrm{m}^{-1}$, $I_{\mathrm{sat}} = 21.849\ \mathrm{kW/cm}^2$.

Figure 4 shows the distribution of the intensity and out power dependent on M calculated in this way. The output intensity decreases with the increasing M but the width of the exiting zone $(Ma - a)$ increases. At $M_{\mathrm{opt}} = 2.18$, the output power reaches its maximum value.

The resonator extraction efficiency (assuming no absorption loss of the output mirror) η_{r} can be computed as a function of laser medium and resonator parameters,

$$\eta_{\mathrm{r}} = \frac{P_{\mathrm{out}}}{g_0 Lab}, \tag{12}$$

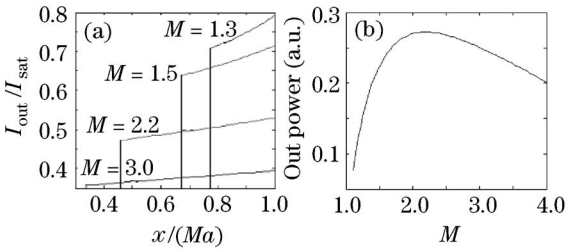

Fig. 4. (a) Distribution of the output intensity over the cross section of the coupling output for the case $g_0L = 1.144$, $\alpha_0 L = 0.0676$. (b) Output power versus magnification M.

where $\eta_r < 1$ is defined as the ratio of the efficiency of a real laser to the efficiency of an ideal laser with $\alpha_0 = 0$ and a very low laser threshold.

The fraction of energy output after one round trip, which is the output coupling δ, is approximately related to the magnification by $\delta = 1 - 1/M$. Figure 5 shows the dependence of the resonator extraction efficiency η_r on $1/M$. At some $M_{opt} = 2.18$, the resonator extraction efficiency reaches its maximum value which is the same as the output power.

It is found that for low M the peaks in the curves are fairly sharp, whereas for large M the peaks are quite gentle, as shown in Fig. 6. This may be understood in terms of the number of transits any ray makes in the resonator; for M near 1, the output coupling is small, and a ray makes many transits between the mirrors before reaching the aperture. Therefore, increasing g_0L slightly increases the total gain path for a ray more for M near 1 than for larger M. Consequently one expects the output

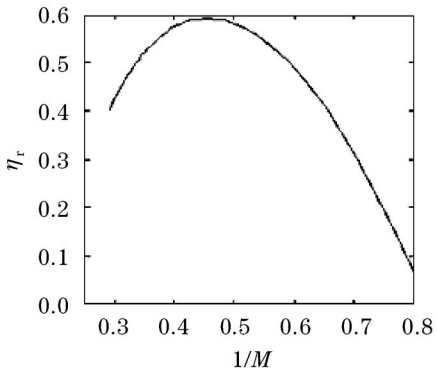

Fig. 5. Dependence of the resonator efficiency η_r on the value $1/M$.

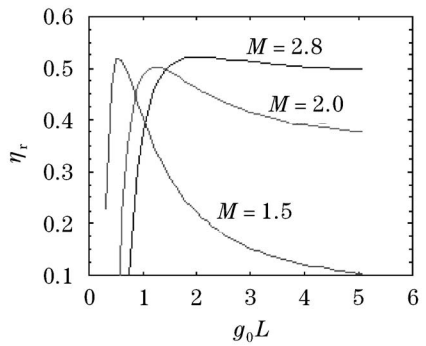

Fig. 6. Dependence of the resonator efficiency η_r on the value g_0L.

power, and so η_r, to be a more sensitive function of g_0L for small values of M than for large values.

The properties of an unstable resonator depend greatly on its equivalent Fresnel number and magnification. So the design parameters for the unstable direction of the stable-unstable resonator are the magnification M and the equivalent Fresnel number N_{eq}. According to Ref. [10], the equivalent Fresnel number of off-axis unstable resonator used in this paper is given by

$$N_{eq} = 4\frac{M-1}{2M^2}N_0. \tag{13}$$

In the end, the parameters of the resonator are decided as follows. The dimension of the output coupling mirror is designed to be 4.55×2 (cm) to fit the active medium. In order to meet the requirement of N_{eq} and experiment, the length is 324.9 cm, and N_{eq} is 1418.5. According to the confocal condition and the definition of the magnification of confocal unstable resonator, the radius of curvature of the output coupling mirror is -550.7 cm, and that of curvature of the second mirror is 1200.5 cm. According to Ref. [11], in order to keep the resonator symmetrical, the distance from the slab to the corresponding mirror is 30.15 cm, and the distance between two slabs is 39.7 cm.

Based on the Fox and Li approach[12], mode properties of off-axis one-sided hybrid resonators are discussed. In our design, the temperature gradient is forced to be nearly one-dimensional, that is to say, there is no thermal effect in the unstable plane; in the other stable plane there is thermal lensing effect.

The unstable direction intensity profiles on the feedback mirror plane for the unloaded and loaded off-axis one-sided hybrid resonator are shown in Fig. 7. The near-field intensity distribution of loaded case is more uniform owing to gain by comparison between Figs. 7(a) and (b). Due to the losses at the optical axis, the intracavity field drops in this region significantly. Thus the intensity distribution is nonuniformity and increases gradually from optical axis to the coupling edge. Therefore, the intensity at the output aperture is higher than the average intensity in the resonator, as increases the output coupling which is defined as the ratio between the power extracted from the coupling aperture and total power travelling towards the feedback mirror. But in loaded case, saturable gain will reduce output coupling towards the geometric value.

The near-field phase distribution and far-field intensity distribution of off-axis one-sided unstable resonator

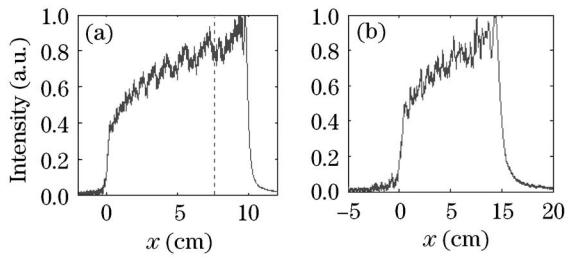

Fig. 7. Near-field unloaded (a) and loaded (b) intensity profiles on the feedback mirror in unstable-direction of unloaded hybrid resonator. The vertical line in (a) indicates the location of the coupling edge.

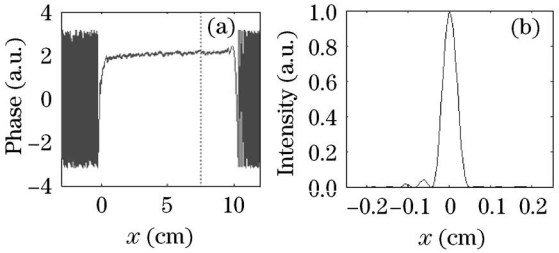

Fig. 8. Near-field phase distribution (a) and far-field intensity distribution (b) of off-axis one-sided unstable resonator.

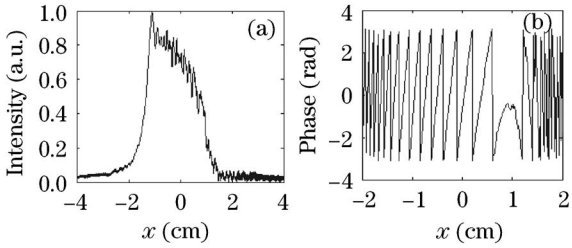

Fig. 9. Near-field intensity (a) and phase (b) profiles in stable direction of normal loaded hybrid resonator with 0.1λ wavefront distortion.

are shown in Fig. 8. The near-field phase is close to uniform in the geometrical edge ($0 < x < 10$ cm). So the far-field intensity distribution of off-axis one-sided case, which merely contains several small side lobes on the left, is relatively smooth.

In stable direction, if there is no thermal distortion, the near-field intensity distribution should be Guassian and the phase be close to uniform in the geometrical edge ($-1 < y < 1$ cm). The wavefront distortion caused by the quasi-one-dimensional thermal gradient seriously influences mode properties in this direction, as can be seen in Fig. 9, which shows the near-field intensity and phase distribution in stable direction of the normal dual-slab laser with off-axis hybrid resonator when wavefront distortion is 0.1λ. It is found that when the wavefront distortion works, intensity shape becomes distorted and a converged solution is not obtained after hundreds of iterations, indicating the presence of strong resonator mode competition, and the phase profile becomes distorted too. These changes degrade the output beam quality, as

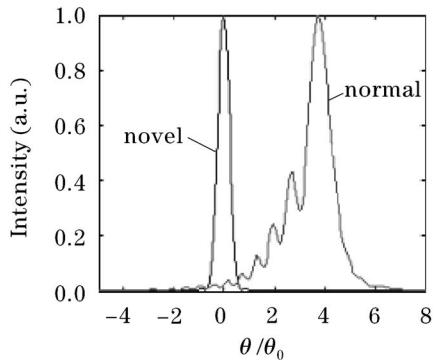

Fig. 10. Far-field intensity profile in stable direction of normal and novel loaded hybrid resonator with 0.1λ wavefront distortion.

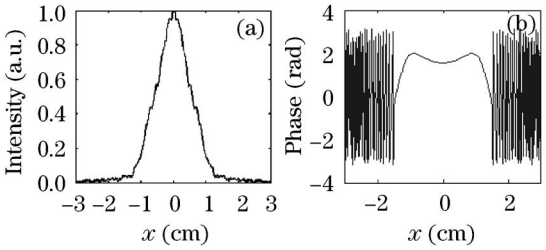

Fig. 11. Near-field intensity (a) and phase (b) profiles in stable direction of novel loaded hybrid resonator with 0.1λ wavefront distortion.

shown in Fig. 10. In contrast with the mode properties of the normal dual-slab laser, the corresponding mode properties of our novel dual-slab laser is shown in Fig. 11. As can be seen, the change of the near-field intensity and phase distribution is slightly because the wavefront distortion is compensated. Therefore, the output beam quality still remains good, as shown also in Fig. 10.

In this paper, we develop the output power and extraction efficiency equation of an off-axis one-sided stable-unstable resonator. By calculation according to these equations, the optimum parameters of resonator are given. At the same time, the near-field and far-field characteristics of the novel dual-slab laser with such resonator have been investigated. By comparing the novel dual-slab laser with the normal dual-slab laser, the novel dual-slab laser presented in this paper realizes the compensation for thermal distortion to some extent by flipping the optical beam and improves the optical beam quality. Therefore, the novel dual-slab laser promises highly efficient laser operation at good beam quality. The related experiments are going on, and the experimental results will be reported later.

L. Zhang's e-mail address is dthyzhll@163.com.

References

1. P. E. Jackson, H. J. Baker, and D. R. Hall, Appl. Phys. Lett. **54,** 1950 (1989).
2. K. Kuba, T. Yamamoto, and S. Yagi, Opt. Lett. **15,** 121 (1990).
3. P. Shi, D. Li, H. Zhang, Y. Wang, and K. Du, Opt. Commun. **229,** 349 (2004).
4. J. Meng, Y. Huang, W. Chen, and Q. Hu, Acta Opt. Sin. (in Chinese) **25,** 1658 (2005).
5. A. E. Siegman, Proc. IEEE **53,** 277 (1965).
6. W. W. Rigrod, IEEE J. Quantum Electron. **14,** 377 (1978).
7. G. T. Moore and R. J. McCarthy, J. Opt. Soc. Am. **67,** 221 (1977).
8. W. W. Rigrod, J. Appl. Phys. **36,** 2487 (1965).
9. G. M. Schindler, J. Quantum Electron. **16,** 546 (1980).
10. J. F. Perkins and C. Cason, Appl. Phys. Lett. **31,** 198 (1977).
11. Y. Liao, H. He, Y. Li, S. Gu, and Z. Wang, Acta Opt. Sin. (in Chinese) **13,** 107 (1993).
12. A. G. Fox and T. Li, Proc. IEEE **51,** 80 (1963).